

PAPER • OPEN ACCESS

## Nanocluster glass-formation: a potential energy landscape perspective

To cite this article: D Y Sun and X G Gong 2020 *New J. Phys.* **22** 103020

View the [article online](#) for updates and enhancements.

### Recent citations

- [Dynamic Crossover in Metallic Glass Nanoparticles\\*](#)  
Shan Zhang *et al*



## PAPER

## Nanocluster glass-formation: a potential energy landscape perspective

## OPEN ACCESS

RECEIVED  
3 May 2020REVISED  
27 September 2020ACCEPTED FOR PUBLICATION  
29 September 2020PUBLISHED  
12 October 2020

Original content from  
this work may be used  
under the terms of the  
[Creative Commons  
Attribution 4.0 licence](#).

Any further distribution  
of this work must  
maintain attribution to  
the author(s) and the  
title of the work, journal  
citation and DOI.

D Y Sun<sup>1,2</sup>  and X G Gong<sup>2,3,\*</sup><sup>1</sup> School of Physics and Electronic Science, Engineering Research Center for Nanophotonics & Advanced Instrument, Ministry of Education, East China Normal University, No.500, Dongchuan Road, Shanghai 200241, The People's Republic of China<sup>2</sup> Key Laboratory for Computational Physical Sciences (MOE), State Key Laboratory of Surface Physics, Department of Physics, Fudan University, Shanghai 200433, The People's Republic of China<sup>3</sup> Collaborative Innovation Center of Advanced Microstructures, Nanjing 210093, The People's Republic of China

\* Author to whom any correspondence should be addressed.

E-mail: [xggong@fudan.edu.cn](mailto:xggong@fudan.edu.cn)**Keywords:** glass transition, molecular dynamics simulations, potential energy landscape, nano systems

## Abstract

The intrinsic nature of glass states or glass transitions has been a mystery for a long time. Recent studies have suggested that glass-formation versus crystallization occurs for potential energy landscapes (PEL) having a specific structure and the present work is an elaboration of this perspective. To explore how the flatness of the PEL related to glass transition, we develop a method to adjust the PEL in a controllable manner. We demonstrate that a relatively flat PEL is not only necessary but also sufficient for the formation of a nanoscale glass. We show that: (1) as long as a nanocluster is located in a region of PEL with local minimum deep enough, it can undergo an abrupt thermodynamic transition reminiscent of the first order transition of bulk materials; and (2) if a nanocluster is located in a relatively flat PEL, it can undergo a very broad transition in their dynamics and thermodynamics that resembles glass-formation in bulk materials in many ways. All these transitions are independent of its structure symmetry, order or disorder. Our simulations also uncover the direct transition from one potential energy minimum to another below the glass transition temperature, which is the consequence of flat PELs.

## 1. Introduction

Potential energy landscapes (PELs) provide a unique perspective and indispensable physical picture for exploring the nature of glass and glass transitions [1–6]. The concept of a PEL comes from Goldstein's seminal paper, in which he made a direct connection between glass transitions and PELs [7]. Later, by introducing the inherent structure, Stillinger and Weber further developed the concept of a PEL and established a statistical mechanics framework for a quantitative calculation of thermodynamic properties of glasses [8]. In the past half century, the PEL of some glasses has been investigated [9–45]. Scientists are trying to correlate the properties of glasses with the PEL. For example, scientists have explicitly proposed a connection between the topology of the PEL (namely the density of configurational states) and the fragility of the associated liquid [46–48]. One breakthrough could be the recognition that the glass transition is rooted in a specific PEL. The PEL of glasses is made up of many metabasins, which are separated by higher barriers [49–54]. In a metabasin, the PEL is relatively flat, even below the glass transition temperature, the system has enough probability jumping from one configuration to another. It was suggested that  $\beta$  relaxation relates to the atomic motion in a metabasin, and  $\alpha$  relaxation is the result of inter-metabasin motion [55, 56]. With metabasins, the excess configuration entropy, as well as the cooperative motion of the Adam–Gibbs's model [57], may be given a reasonable explanation [58, 59].

With the help of the PEL viewpoint, it seems that we are approaching understanding the nature of glasses. The straightforward way to address these problems is to investigate how thermodynamic behavior changes with variations of the PEL. However, it is not easy to adjust PELs, especially in a controlled manner. There have been a few attempts to study the glass state by adjusting PELs. In these studies, PELs were mostly

manipulated by simply changing one parameter of model potentials [60–66]. One obvious disadvantage of the method lies in that the relationship between PELs and the potential parameters is elusive. Especially since the PEL is a complex function in high-dimensional phase space, it seems impossible to establish this kind of relationship, even though previous studies still presented fruitful and instructive results.

In order to establish a relationship between PEL and glass transitions as direct as possible, we propose a controlled manner to adjust  $3N$ -dimensional PELs, where  $N$  is the number of atoms. By directly adjusting  $3N$ -dimensional PELs, we have systematically studied the glass transition in a few nanoclusters, both ordered and disordered.

For a long time, there are two parallel themes in the study of glasses, namely bulk glasses and nanoscale glasses. These two themes mutually support and complement, providing different but very important perspectives for exploring the nature of glasses. In addition to its own scientific and technological importance, studies on nanoscale glass has many advantages. As demonstrated previously, the ground state structure of some clusters is glassy [67, 68]. For nanoclusters containing dozens of atoms, the simulation time at the interested temperature range can be more than thousands of times the relaxation time. This point allows us to study the thermodynamic behavior of glass transitions independent of the cooling rate. It becomes possible to explore the typically slow dynamics of glasses around the glass transition temperature. These advantages are not available in bulk glass [69–71].

In this work, we establish the direct relationship between PELs and the glass transition in nanoscale, and found that an enough flat PEL is the key feature for a glass transition, while the symmetry is not direct issue.

## 2. Methodological development

In order to adjust the  $3N$ -dimensional PEL, we propose the following approach. Assuming  $\varphi(r_1, r_2, \dots, r_N)$  is the total potential energy of a system. In most molecular dynamics (MD) simulations,  $\varphi(r_1, r_2, \dots, r_N)$  is usually expressed as a sum over specific interatomic potentials. Obviously  $\varphi(r_1, r_2, \dots, r_N)$  defines the  $3N$ -dimensional PEL of systems. It needs to point out that our modification is applied to PEL, rather than the free energy landscape (FEL). Different from FEL, PEL itself does not depend on temperature.

We define a new potential energy  $\varphi^*$  as,

$$\varphi^* = \begin{cases} \varphi + \varepsilon(\varphi - \varphi_0)^m & \text{for } \varphi \leq \varphi_0 \\ \varphi & \text{for } \varphi > \varphi_0 \end{cases}, \quad (1)$$

where  $\varepsilon, \varphi_0$  are adjustable parameters and  $m$  is an even number ( $m \geq 2$ ). Thus  $\varphi^*$  defines a new  $3N$ -dimensional PEL.

It is easy to calculate the PEL difference between  $\varphi^*$  and  $\varphi$  in the phase space by directly using equation (1). Since

$$\frac{\partial \varphi^*}{\partial r_i} = (1 + \varepsilon m(\varphi - \varphi_0)^{m-1}) \frac{\partial \varphi}{\partial r_i} \quad (2)$$

we see that all extreme and saddle points of  $\varphi$  pass to  $\varphi^*$ , keeping their locations in phase space unchanged. In addition,  $\varphi^*$  has new extreme points or saddle points determined by

$$1 + \varepsilon m(\varphi_s - \varphi_0)^{m-1} = 0. \quad (3)$$

As we show below, one can carefully select the parameters  $(\varphi_0, m, \varepsilon)$ , to ensure these additional extreme or saddle points are far away from the temperature region where we are interesting.

The PEL described by equation (1) is adjusted in the following two aspects. First, suppose  $\varphi_a$  and  $\varphi_b$  ( $\varphi_a < \varphi_b \leq \varphi_0$ ) being adjacent minimum and maximum points at the PEL of  $\varphi$  respectively, and  $\varphi_a^*$  and  $\varphi_b^*$  being the counterparts at the PEL of  $\varphi^*$ , we have  $\varphi_b^* - \varphi_a^* = \varphi_b - \varphi_a + \varepsilon(\varphi_b - \varphi_0)^m - \varepsilon(\varphi_a - \varphi_0)^m$ . Thus, if  $\varepsilon$  is negative (positive), the barrier in PEL becomes higher (lower). Second, from the second derivatives of the potential energy with respect to atomic positions, namely

$$\frac{\partial^2 \varphi^*}{\partial r_i \partial r_j} = \frac{\partial^2 \varphi}{\partial r_i \partial r_j} + \varepsilon m(\varphi - \varphi_0)^{m-1} \frac{\partial^2 \varphi}{\partial r_i \partial r_j} + (\varepsilon m(m-1)(\varphi - \varphi_0)^{m-2}) \frac{\partial \varphi}{\partial r_i} \frac{\partial \varphi}{\partial r_j}.$$

At any extreme point or saddle point, i.e.,  $\frac{\partial \varphi}{\partial r_i} = 0$  or  $\frac{\partial \varphi}{\partial r_j} = 0$ , we have

$$\frac{\partial^2 \varphi^*}{\partial r_i \partial r_j} = \frac{\partial^2 \varphi}{\partial r_i \partial r_j} (1 + \varepsilon m(\varphi - \varphi_0)^{m-1}). \quad (4)$$

one can see that, compared to that of  $\varphi$ , the PEL of  $\varphi^*$  at extreme points can be adjusted to be more or less flat, based the choice of  $\varepsilon$ ,  $\varphi_0$  and  $m$ . For example, if  $\frac{\partial^2 \varphi}{\partial r_i \partial r_j} > 0$ , by taking  $(1 + \varepsilon m(\varphi - \varphi_0)^{m-1}) > 0$  the PEL of  $\varphi^*$  will become steeper. From the above two points, we can see that, we are able to not only directly adjust the height of the barrier (the first point), but also adjust the second derivative of the PEL (the steepness of PELs) near the extreme point (the second point). Thus, we can conclude that the flatness of PELs can be adjusted by changing  $\varepsilon$ . Here the *flatness* of PELs refers a measure of barriers heights in PELs.

It needs to point out that, by adjusting PELs, other than the additional extreme or saddle points determined by equation (3), we do not change either the number or position of extreme points in phase space, which is a remarkable feature of our method. This statement is easy to see from equation (2), namely, except the additional extreme points determined by equation (3), as long as the first derivative of  $\varphi$  is zero, does the first derivative of  $\varphi^*$ . We note that, similar ideas have been used to study the dynamics of polymers [72–74] as a mechanism of accelerating molecular dynamic simulations.

Using MD simulations, we have studied the melting behavior of two aluminum nanoclusters ( $\text{Al}_{43}$  and  $\text{Al}_{55}$ ). The interaction between Al atoms is described by the glue potential [75] (**Note: the total potential energy ( $\varphi$ ) discussed above is not the interatomic potential.  $\varphi$  is a sum of the total interaction energy among atoms**). It is known that, at  $\varepsilon = 0$   $\text{Al}_{43}$  has a disordered ground state structure [67]. The ground state of  $\text{Al}_{55}$  has an ordered structure with high symmetry ( $I_h$  symmetry) [76]. The melting of  $\text{Al}_{55}$  is a typical solid-liquid phase transition, while  $\text{Al}_{43}$  melts and solidifies with a typical glass-like transition, which has been suggested to be an ideal glass [68]. The similar glass-like transition was observed in some Al clusters experimentally [77].

In current studies, for  $\text{Al}_{43}$ ,  $\varphi_0$  and  $m$  are  $-2.58 \times 43$  eV and 6, respectively, and  $\varepsilon$  is chosen in the range of  $(-4 \times 10^{-5}, 0)$ . Since here  $\varepsilon$  is negative, the PEL becomes steeper as  $\varepsilon$  is decreased. For  $\text{Al}_{55}$ ,  $\varphi_0 = -2.58 \times 55$  eV,  $m = 4$ , and  $\varepsilon$  is in the range  $(0.0, 2.8 \times 10^{-4})$ . Since here  $\varepsilon$  is positive, the PEL becomes flatter as  $\varepsilon$  is increased. Our simulations confirm that for all chosen  $\varepsilon$ , the disordered structure and  $I_h$  structure are still the stable configurations for  $\text{Al}_{43}$  and  $\text{Al}_{55}$ , respectively.

For both nanoclusters,  $\varphi_0 = -2.58$  eV times the number of atoms, corresponds to the total potential energy above the melting temperature of  $\varepsilon = 0$ . It is easy to calculate that the additional extreme or saddle points determined by equation (3) are far away from the potential range of interest. The value of  $\varphi_s$  is easily gotten from equation (3). For  $\text{Al}_{43}$ ,  $\varphi_s > \varphi_0$ , and the corresponding  $\varphi_s$  for all  $\varepsilon$  is higher than 900 K, which is irrelevant to any phase or glass transition in the current studies. For  $\text{Al}_{55}$ ,  $\varphi_s < \varphi_0$ , for all studied  $\varepsilon$ , and the corresponding temperature is less than  $\sim 200$  K, which is much lower than the melting point or glass transition temperatures. In fact, the extra extreme or saddle points at  $\varphi_s$  have essentially no effect on the thermodynamic properties.

### 3. Result and discussion

The basic difference between a glass transition and a solid–liquid phase transition lies in how the energy and volume change with  $T$ . In a glass transition process, both energy and volume change continuously over the whole range of temperatures. While in a solid–liquid phase transition, both total energy (kinetic plus potential energy) and volume have a jump at the melting temperature [78]. Figures 1 and 2 depict the change of total energies, volumes and specific heats with temperature for different PELs adjusted by different parameters. The melting behavior is closely related to the flatness of the PEL regardless of the structural symmetry. For the disordered  $\text{Al}_{43}$ , with the increase of  $\varepsilon$ , for which the PEL becomes steeper and steeper, the melting behavior changes accordingly from a typical glass transition to a first order solid–liquid phase transition. Strictly speaking, a true thermodynamics phase transition could not occur in a nanocluster. In this paper, the first order phase transition refers a rather abrupt thermodynamic transition reminiscent of the first order phase transition of bulk materials, while the glass transition refers a very broad transition in thermodynamics that resembles glass transition in bulk materials in many ways. For the ordered  $\text{Al}_{55}$ , when the PEL gets progressively flatter by increasing  $\varepsilon$ , the melting behavior changes from a typical first order solid–liquid phase transition to a glass transition. These results indicate that the glass transition is not intrinsically dependent on the structural symmetry, but on the flatness of a PEL. When the PEL becomes steeper, a first order solid–liquid phase transition occurs; when the PEL becomes flatter, a glass transition occurs.

At  $\varepsilon = 0$ , the melting of  $\text{Al}_{43}$  is a typical glass transition, indicated by the continuous change in energy (black circles in upper panel of figure 1) and volume (black circles in upper panel of figure 2), as we have demonstrated several times in our previous work [79, 80]. The glass transition temperature, which is around 520 K, can be estimated by a linear extrapolation of the low temperature and high temperature dependence of energies. As  $\varepsilon$  decreases from zero to negative, which means the PEL gets steeper and steeper,

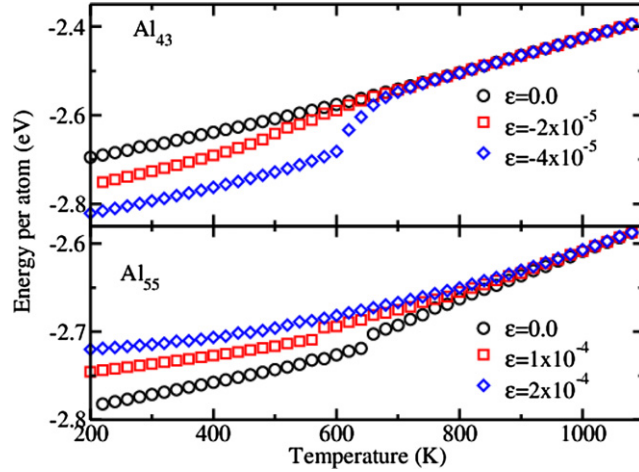


**Figure 1.** The energy as a function of temperature for ordered  $\text{Al}_{55}$  (lower panel) and disordered  $\text{Al}_{43}$  (upper panel). For  $\text{Al}_{43}$ , with the increase of  $\varepsilon$ , the continuous change in energy is gradually replaced by a step, while for  $\text{Al}_{55}$ , with the increase of  $|\varepsilon|$ , a step in energy is gradually replaced by a continuous change.

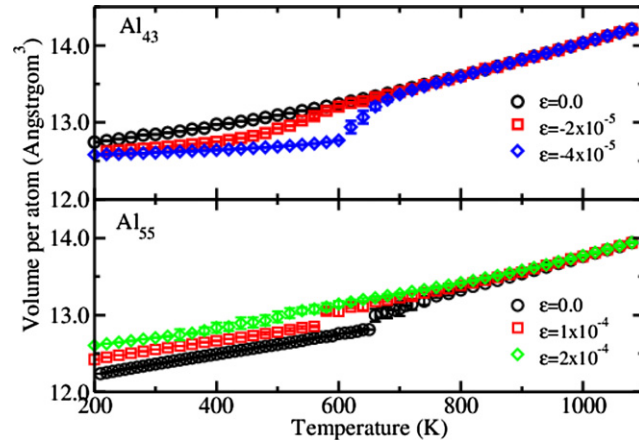


**Figure 2.** The volume as a function of temperature for ordered  $\text{Al}_{55}$  (lower panel) and disordered  $\text{Al}_{43}$  (upper panel). The change in volume is similar to that shown in figure 1.

the melting of  $\text{Al}_{43}$  shows a typical first order solid–liquid phase transition of finite systems, as shown in figure 1 (upper panel). For  $\varepsilon = -2 \times 10^{-5}$ , the melting of  $\text{Al}_{43}$  has begun to deviate from the glass transition behavior. For  $\varepsilon = -4 \times 10^{-5}$ , the energy changes rapidly, and a significant latent heat appears. The step around melting is not very sharp, which is a remarkable feature of the finite size effect of melting [81]. The clear fact beyond question is that a typical first-order phase transition does occur in this disordered glass-like  $\text{Al}_{43}$  after the PEL is adjusted, i.e., if the PEL of glass becomes deeper, it shows a typical solid-liquid transition.

The lower panel of figure 1 shows the energy as a function of temperature for the ordered  $\text{Al}_{55}$  with a range of  $\varepsilon$ . The energy has a clear step for  $\varepsilon = 0.0$  and  $1 \times 10^{-4}$  at the melting temperature, a typical feature of a first-order phase transition. However, for  $\varepsilon = 2 \times 10^{-4}$ , the energy step disappears, resulting in a typical glass transition process. This indicates that, if an ordered nanocluster is trapped in a relatively flat PEL, a glass transition can occur.

The change of volume with temperature further supports our conclusions drawn from energy changes. Figure 2 shows the volume as a function of temperature for  $\text{Al}_{43}$  (upper panel) and  $\text{Al}_{55}$  (lower panel). For the disordered  $\text{Al}_{43}$ , when  $\varepsilon = 0$ , the volume changes continuously with typical glass transition characteristics. When  $\varepsilon = -5 \times 10^{-5}$ , the volume jumps obviously at the melting point, showing characteristics typical of a solid–liquid phase transition in finite systems. For ordered  $\text{Al}_{55}$ , the volume clearly jumps for  $\varepsilon = 0$  and  $1 \times 10^{-4}$  around the melting temperature. This is a typical feature of a first-order phase transition. When  $\varepsilon = 2 \times 10^{-4}$ , the step has disappeared, reflecting a typical glass transition process.

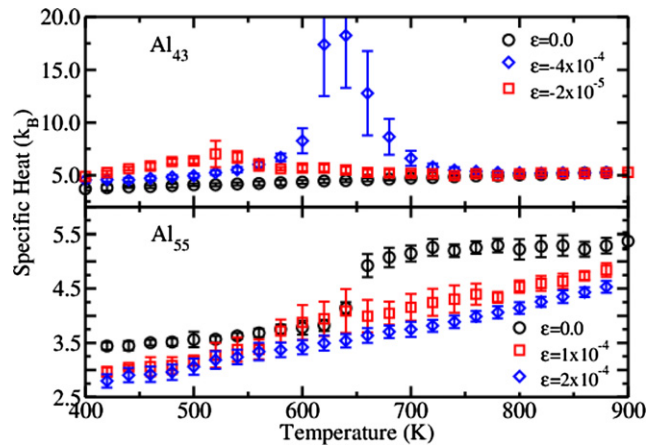


**Figure 3.** The specific heat as a function of temperature for disordered nanocluster  $\text{Al}_{43}$  (lower panel) and ordered nanocluster  $\text{Al}_{55}$  (upper panel). For  $\text{Al}_{43}$ , with the decrease of  $\varepsilon$ , i.e., the PEL becomes deeper, the peak in specific heat becomes sharper and sharper, indicating evolution from a glass transition to a first order phase transition. For  $\text{Al}_{55}$ , with the increase of  $|\varepsilon|$ , i.e., the PEL becomes flatter, the jump in specific heat disappears gradually, indicating evolution from a first order phase transition to a glass transition.

The change in melting behavior for different PELs can also be found from specific heat, as shown in figure 3. For  $\text{Al}_{43}$  (lower panel of figure 3), for  $\varepsilon = 0$  the specific heat does not exhibit any peak or discontinuity, indicating a typical glass transition. With  $\varepsilon = -2 \times 10^{-5}$ , the peak in specific heat becomes sharp, which is a distinct feature of melting in finite-size systems. The appearance of a peak instead of a discontinuity is due to the existence of the solid–liquid coexistence for finite-size systems. For  $\text{Al}_{55}$  (upper panel of figure 3), we have identified a change from the first-order solid–liquid phase transition to the glass transition as the PEL getting flatter and flatter. One can see that, for  $\varepsilon = 0$  and  $1 \times 10^{-4}$ , the specific heat has a step at the melting point, which is a hallmark of solid–liquid phase transitions. While it becomes a continuous change and does not show any peak in the entire temperature range for  $\varepsilon = 2 \times 10^{-4}$ , implying a glass transition.

Principal radii of gyration, in addition to indicating a change of nanocluster shape, also identify the type of phase transition. We find that the difference between the maximum and minimum radius of gyration ( $\Delta R = R_{\max} - R_{\min}$ ) gives clear information about structural changes and melting behavior. Figure 4 shows  $\Delta R$  as a function of temperature. For a first order solid–liquid phase transition ( $\text{Al}_{43}$  with  $\varepsilon = -3.4 \times 10^{-5}$ ,  $\text{Al}_{55}$  with  $\varepsilon = 1.0 \times 10^{-4}$ ), the nanoclusters keep their original structure before completely melting, indicated by an approximately constant value of  $\Delta R$ . A jump in  $\Delta R$  around the melting temperature can be clearly seen for these nanoclusters. For a typical glass transition ( $\text{Al}_{43}$  at  $\varepsilon = -0.4 \times 10^{-5}$ ,  $\text{Al}_{55}$  at  $\varepsilon = 2.0 \times 10^{-4}$ ), far below  $T_g$ ,  $\Delta R$  has already begun to change. With the increase of temperature, in contrast to the first solid–liquid phase transition,  $\Delta R$  gradually changes, spanning temperatures over a range of about 200 K. We can define the temperature at which nanoclusters begin to change shape as the starting temperature ( $T_s$ ), which represents a characteristic temperature, above which configurational entropies emerge in glassy states.

According to figure 4, three characteristic temperatures,  $T_s$ ,  $T_g$  and  $T_m$ , can be determined.  $T_m$  is the obvious one without any ambiguity. It is defined as the temperature, at which  $\Delta R$  jumps, which is in accordance with abrupt changes in the volume and energy as shown in figures 1 and 2.  $T_s$  can be easily defined as the temperature at which  $\Delta R$  obviously begins to change. In contrast, it is not easy to determine  $T_g$ , which is a well-known difficulty. However, figure 4 shows us that the glass transition is much more clearly reflected on the  $\Delta R$ – $T$  curve. In the current work,  $T_g$  can be estimated by linear extrapolation of the low temperature and high temperature dependence of  $\Delta R$ , as illustrated by dash lines in figure 4. Two issues need to be emphasized: (1)  $T_g$  is consistent with that determined by other thermodynamic quantities, energies, volumes, etc; and (2) it is inevitable that there can be large errors, as is also the case in other methods.

There seems to be a consensus that cooperative diffusion within a few atoms exists in a glass. This perspective comes from Adam–Gibbs entropy theory and Goldstein’s PEL picture [7, 57]. Recently, it has become generally believed that this cooperative diffusion may correspond to a transition in a metabasin. We show that the atomic diffusion in a glass below  $T_g$  can indeed be considered as a transition from one potential energy minimum to another, for which the transition is accomplished by cooperative motion [82–86].



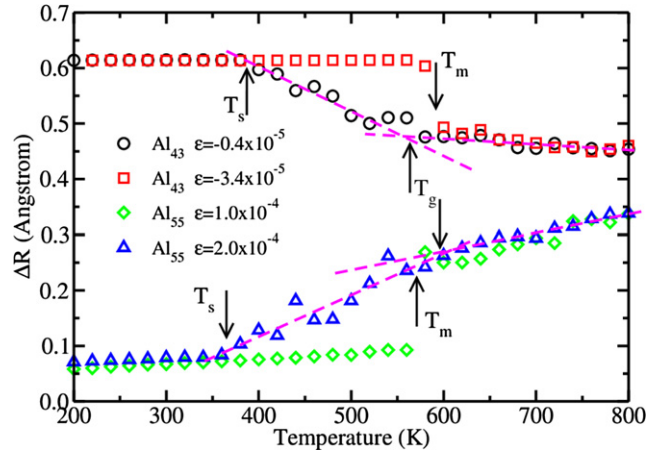


Figure 4. The difference between the maximum and minimum radius of gyration.

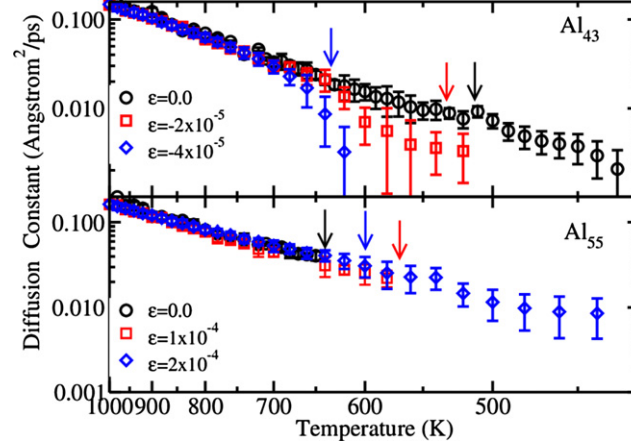


Figure 5. Temperature dependence of the diffusion constant for  $\text{Al}_{43}$  (upper panel) and  $\text{Al}_{55}$  (lower panel), where the vertical axis is logarithmic and the horizontal axis is reciprocal scale. For  $\text{Al}_{43}$  at  $\varepsilon = 0.0$  and  $\text{Al}_{55}$  at  $\varepsilon = 2 \times 10^{-4}$ , there is the evident diffusivity below the glass transition temperature. The arrows, with the same color as data points, roughly indicate the corresponding  $T_g$  or  $T_m$ .

We have calculated the self-diffusion coefficient, which is shown in figure 5 for  $\text{Al}_{43}$  (upper panel) and  $\text{Al}_{55}$  (lower panel). If nanoclusters melt through a solid–liquid phase transition, the atomic diffusivity becomes negligible below the melting point, indicating a normal solid state. For both  $\text{Al}_{43}$  and  $\text{Al}_{55}$ , if a glass transition occurs, the atoms have obvious diffusivity below  $T_g$ . This is a typical feature for glassy nanoclusters suggested recently [79, 80]. Although these data in figure 5 might have uncertainty somehow, it is clear that, within the error bar, these data cannot be fitted to a single Arrhenius curve. However, two Arrhenius curves can make the high temperature and low temperature data well fitted.

The diffusion activation energy can be obtained by fitting the diffusion coefficient via temperatures. For glass transitions, diffusion activation energies are clearly different below and above  $T_g$ . As we have pointed out previously, this is a typical characteristic of diffusion in glasses [79, 80]. It is well known that the diffusion of atoms in liquids is mainly determined by thermal collisions. The change in activation energy around  $T_g$  may imply a change of diffusion mechanism or the emergence of some new modes for atom displacements. As discussed in detail in our previous works, diffusion involves a kind of cooperative motion for which the diffusion barrier is surprisingly lower than that in the liquid at high temperatures [80]. The similar change in the activation energy has been found in other systems when cooperative diffusions occur [87, 88].

Obviously, this cooperative diffusion is the result of a relatively flat PEL, because it only occurs with a sufficiently flat PEL, i.e.,  $\varepsilon \geq -1 \times 10^{-5}$  for  $\text{Al}_{43}$  and  $\varepsilon \geq 2 \times 10^{-4}$  for  $\text{Al}_{55}$ . One can conclude that the relatively flat PEL is the essence of the glassy state, and results in cooperative diffusion at low temperature.

This cooperative diffusion corresponds to a jump from one local minimum to a neighboring local minimum, still in the relatively flat PEL. The direct way to show this is to calculate the evolution of total

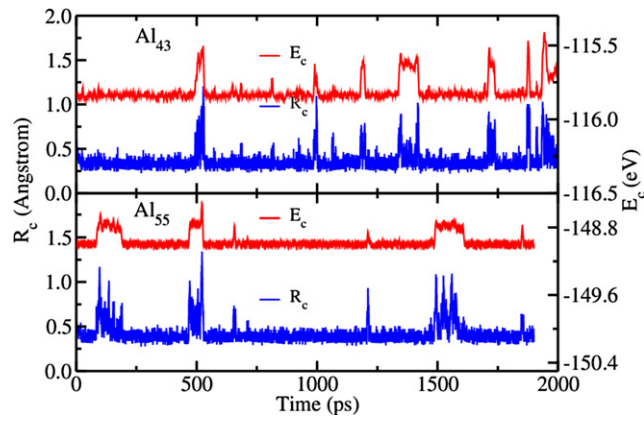


**Figure 6.** The short-time average of potential energy ( $E_c$ ) and displacement ( $R_c$ ) for  $\text{Al}_{43}$  at  $\varepsilon = 0.0$  (upper panel) and  $\text{Al}_{55}$  at  $\varepsilon = 2 \times 10^{-4}$  (lower panel), where the temperature is 400 K.

potential energies and atomic displacements. In order to separate the thermal fluctuation from the energy and atomic displacements, the short-time average of the energy ( $E_c(t)$ ) and atomic displacement ( $R_c(t)$ ) are calculated by averaging over a certain time interval. More concretely, the short-time average of displacement is

$$R_c(t) = \left( \frac{1}{N} \sum_{i=1}^N (r_i(t) - r_i(t + \Delta t))^2 \right)^{\frac{1}{2}},$$

where  $N$  is the number of atoms,  $r_i(t)$  denotes the position of the  $i$ th atom at time  $t$ , and  $\Delta t$  is a short duration, 5 ps in current studies. Our previous study has shown that  $R_c(t)$  can be used to identify the cooperative motion [79]. The short-time average of the total potential energy is

$$E_c(t) = \frac{1}{\Delta t} \int_0^{\Delta t} E(t + \tau) d\tau,$$

where  $E(t)$  is the instantaneous total potential energy, and  $\Delta t$  is again 5 ps. If  $E_c(t)$  takes a certain value at one time period and is a different value during another time period, the system can be considered to be at different local minimum of the PEL. If  $E_c(t)$  is synchronized with a notable change in  $R_c(t)$ , we can conclude that the cooperative diffusion corresponds to the jump from one PEL minimum to another.

Figure 6 shows the evolution of  $R_c$  and  $E_c$  over time. The upper panel of figure 6 corresponds to  $\text{Al}_{43}$  at  $\varepsilon = 0.0$ , the lower panel of figure 6 corresponds to  $\text{Al}_{55}$  at  $\varepsilon = 2 \times 10^{-4}$ , both at  $T = 400$  K. Both  $E_c$  and  $R_c$  maintain relatively small values over many time periods, which corresponds to one or more equilibrium states with similar energy. However, in some short periods of time,  $R_c$  has a rapid increase. By carefully observing the atomic trajectory, we find that the rapid increase of  $R_c$  is always associated with a larger displacement of a few atoms at the same time. The size of displacement is comparable to the average distance between atoms, indicating that diffusion occurs. This process can be considered as a cooperative diffusion. At the same time, a rapid increase of  $E_c$  occurs simultaneously, which should relate to the activation process of this cooperative diffusion. After a rapid increase,  $R_c$  quickly returns to the smaller value, then  $E_c$  equilibrates to a new state. Perhaps it corresponds to a transition from one inherent structure to another. Since the two equilibrium states are very close in energy, which is precisely what people speculate or assume about a metabasin. Although only a few cooperative diffusion events are shown, such behaviors are common in glassy states. The cooperative diffusion behavior observed in our simulations is similar to what described in other clusters [89, 90]. It was found that, there is a critical cluster size for which the cooperative motion occurs throughout the cluster, while for larger clusters, the cooperative motion is confined to an interfacial region [89, 90].

Combining the current result with our previous work [79], we suggest a general scenario for the different stages of glass-formation. Thermodynamically, a solid, glass and liquid mainly differ in two aspects, internal energies and configurational entropies. The difference in energies is obvious and easily understood. However, the difference in configurational entropies is ambiguous. A solid is in a deep potential well, in which the vibrational entropy is important, while the configurational entropy is neglectable. In liquids, the atoms diffuse quickly, the configurational entropy reaches a maximum compared to solids and glasses. In glasses, the atom vibrates at a local potential minimum for most of the time. As we have demonstrated, the remarkable feature of glasses is the existence of collective diffusion, thus the



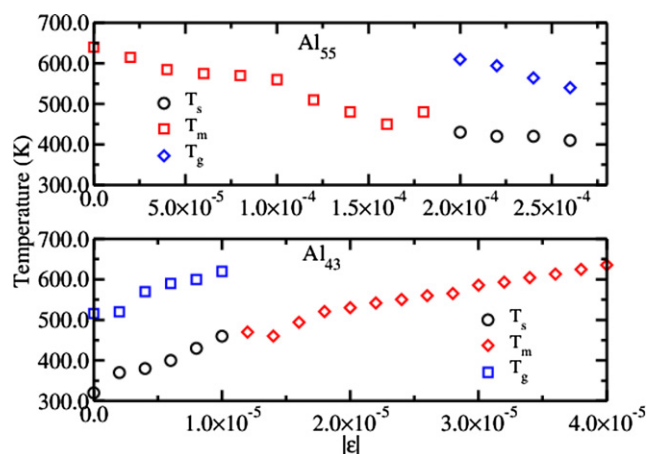


**Figure 7.**  $T_s$ ,  $T_g$  and  $T_m$  as a function of  $\varepsilon$ . For  $\text{Al}_{43}$ ,  $\varepsilon < -1 \times 10^{-5}$ , the disordered nanoclusters begin to exhibit a first-order solid–liquid phase transition. For  $\text{Al}_{55}$ ,  $\varepsilon > 2 \times 10^{-4}$ , the ordered nanoclusters begin to undergo a glass transition.

configurational entropy should play a role on the thermodynamics behavior of glasses. The measured vibrational entropies of the glass and liquid show a tiny excess over the crystal, representing less than 5% of the total excess entropy measured with step calorimetry. A recent experiment has also shown that the excess entropy of metallic glasses is almost entirely configurational in origin [91].

By adjusting the PEL, we are able to make some comprehensive comparisons. Figure 7 shows the change of  $T_s$ ,  $T_g$  and  $T_m$  as a function of  $\varepsilon$ . It can be seen that,  $T_g$ , for either  $\text{Al}_{43}$  or  $\text{Al}_{55}$ , shows a significant jump when the melting behavior of the nanocluster changes from a first-order solid–liquid phase to a glass transition. This jump should be caused by the emergence of configuration entropies.

Finally, although the glass transition in nanoclusters described in our work and others is not identical in all details with macroscopic glass transition, they do share many similarities. They should have the similar, even the same, thermodynamic roots, which is what we want to emphasize. Additionally, our current research could also shed light on micelle formation, equilibrium polymerization and other self-assembly processes etc.

## 4. Summary

In this paper, we have systematically studied the glass transition of nanoclusters by molecular dynamics. We have proposed a new method to adjust the flatness of a potential energy landscape. This method can adjust the height of potential barriers without changing the number or position in phase space of the potential energy extremal points. By adjusting the flatness of the potential energy landscape, we have found that the nanoclusters can undergo either a first-order solid–liquid phase transition or a glass transition, which is independent of the structural symmetry. This makes it possible for us to demonstrate for the first time that a relatively flat potential energy landscape is an intrinsic nature for glass transitions. Because these nanoclusters undergo an apparently equilibrium glass transition, i.e. corresponding to an arbitrarily slow cooling rate, it allows the study of the dynamic processes at any long time. We find that, even under the glass transition temperature, the system can frequently transfer from one potential surface minimum to another, and this process is achieved by a collective diffusion, which is completely different from the thermal collision process in liquids. Our study provides, for the first time, a microscopic version of atomic motion below the glass transition temperature, as well as a physical picture of the potential energy landscape.

## Acknowledgments

Project supported by the National Natural Science Foundation of China (Grant No. 11874148). The computations were supported by ECNU Public Platform for Innovation.

## ORCID iDs

D Y Sun  <https://orcid.org/0000-0002-9728-8017>

## References

- [1] Debenedetti P G and Stillinger F H 2001 *Nature* **410** 259
- [2] Sciortino F 2005 *J. Stat. Mech.* **P05015**
- [3] Heuer A 2008 *J. Phys.: Condens. Matter.* **20** 373101
- [4] Buchenau U 2003 *J. Phys.: Condens. Matter.* **15** S955
- [5] Raza Z, Alling B and Abrikosov I A 2015 *J. Phys.: Condens. Matter.* **27** 293201
- [6] Berthier L and Biroli G 2011 *Rev. Mod. Phys.* **83** 587
- [7] Goldstein M 1969 *J. Chem. Phys.* **51** 3728
- [8] Stillinger F H and Weber T A 1982 *Phys. Rev. A* **25** 978
- [9] Heuer A 1997 *Phys. Rev. Lett.* **78** 4051
- [10] Sastry S, Debenedetti P G and Stillinger F H 1998 *Nature* **393** 554
- [11] Miller M A, Doye J P K and Wales D J 1999 *J. Chem. Phys.* **110** 328
- [12] Daldoss G, Pilla O, Viliani G, Brangian C and Ruocco G 1999 *Phys. Rev. B* **60** 3200
- [13] Sciortino F, Kob W and Tartaglia P 1999 *Phys. Rev. Lett.* **83** 3214
- [14] Büchner S and Heuer A 2000 *Phys. Rev. Lett.* **84** 2168
- [15] Sastry S 2001 *Nature* **409** 164
- [16] Wales D J and Doye J P K 2001 *Phys. Rev. B* **63** 214204
- [17] Saika-Voivod I, Poole P H and Sciortino F 2001 *Nature* **412** 514
- [18] Middleton T F and Wales D J 2001 *Phys. Rev. B* **64** 024205
- [19] Stillinger F H and Debenedetti P G 2002 *J. Chem. Phys.* **116** 3353
- [20] Grigera T S, Cavagna A, Giardina I and Parisi G 2002 *Phys. Rev. Lett.* **88** 055502
- [21] Angelani L, Ruocco G, Sampoli M and Sciortino F 2003 *J. Chem. Phys.* **119** 2120
- [22] Doliwa B and Heuer A 2003 *Phys. Rev. Lett.* **91** 235501
- [23] Chowdhary J and Keyes T 2004 *J. Phys. Chem. B* **108** 19786
- [24] Saksaengwijit A, Reinisch J and Heuer A 2004 *Phys. Rev. Lett.* **93** 235701
- [25] Vogel M, Doliwa B, Heuer A and Glotzer S C 2004 *J. Chem. Phys.* **120** 4404
- [26] Fyodorov Y V 2004 *Phys. Rev. Lett.* **92** 240601
- [27] Moreno A J, Buldyrev S V, La Nave E, Saika-Voivod I, Sciortino F, Tartaglia P and Zaccarelli E 2005 *Phys. Rev. Lett.* **95** 157802
- [28] Heuer A, Doliwa B and Saksaengwijit A 2005 *Phys. Rev. E* **72** 021503
- [29] Odagaki T, Yoshidome T, Koyama A and Yoshimori A 2006 *J. Non-Cryst. Solids* **352** 4843
- [30] Wang C and Stratt R M 2007 *J. Chem. Phys.* **127** 224504
- [31] Rodríguez Fris J A, Appignanesi G A, La Nave E and Sciortino F 2007 *Phys. Rev. E* **75** 041501
- [32] De Souza V K and Harrowell P 2009 *Phys. Rev. E* **80** 041503
- [33] Rehwald C, Gnan N, Heuer A, Schröder T, Dyre J C and Diezemann G 2010 *Phys. Rev. E* **82** 021503
- [34] Charbonneau P, Kurchan J, Parisi G, Urbani P and Zamponi F 2014 *Nat. Commun.* **5** 3725
- [35] Du X and Weeks E R 2016 *Phys. Rev. E* **93** 062613
- [36] Hwang H J, Riggleman R A and Crocker J C 2016 *Nat. Mater.* **15** 1031
- [37] Jin Y and Yoshino H 2017 *Nat. Commun.* **8** 14935
- [38] Wei Z-Y, Shang C, Zhang X-J and Liu Z-P 2017 *Phys. Rev. B* **95** 214111
- [39] Niblett S P, De Souza V K, Jack R L and Wales D J 2018 *J. Chem. Phys.* **149** 114503
- [40] Blank-Burian M and Heuer A 2018 *Phys. Rev. E* **98** 033002
- [41] Ros V, Ben Arous G, Biroli G and Cammarota C 2019 *Phys. Rev. X* **9** 011003
- [42] Cao P, Short M P and Yip S 2019 *Proc. Natl Acad. Sci. USA* **116** 18790
- [43] Scalliet C and Berthier L 2019 *Phys. Rev. Lett.* **122** 255502
- [44] Deckarm M J, Braun C and Birringer R 2019 *J. Appl. Phys.* **126** 205102
- [45] Han D, Wei D, Cao P-H, Wang Y-J and Dai L-H 2020 *Phys. Rev. B* **101** 014113
- [46] Angell C A 1988 *J. Phys. Chem. Solids* **49** 863
- [47] Angell C A 1991 *J. Non-Cryst. Solids* **131-133** 13
- [48] Scopigno T, Ruocco G, Sette F and Monaco G 2003 *Science* **302** 849
- [49] Vallée R A L, van der Auweraer M, Paul W and Binder K 2006 *Phys. Rev. Lett.* **97** 217801
- [50] Appignanesi G A, Rodríguez Fris J A, Montani R A and Kob W 2006 *Phys. Rev. Lett.* **96** 057801
- [51] Yang Y and Chakraborty B 2009 *Phys. Rev. E* **80** 011501
- [52] Oppelstrup T and Dzugasov M 2009 *J. Chem. Phys.* **131** 044510
- [53] Okushima T, Niiyama T, Ikeda K S and Shimizu Y 2018 *Phys. Rev. E* **97** 021301(R)
- [54] Despa F and Berry R S 2001 *J. Chem. Phys.* **115** 8274
- [55] Goldstein M 2011 *J. Non-Cryst. Solids* **357** 249
- [56] Keys A S, Hedges L O, Garrahan J P, Glotzer S C and Chandler D 2011 *Phys. Rev. X* **1** 021013
- [57] Adam G and Gibbs J H 1965 *J. Chem. Phys.* **43** 139
- [58] Johari G P and Khouri J 2013 *J. Chem. Phys.* **138** 12A511
- [59] Ozawa M, Scalliet C, Ninarello A and Berthier L 2019 *J. Chem. Phys.* **151** 084504
- [60] Jund P, Rarivomanantsoa M and Jullien R 2000 *J. Phys.: Condens. Matter.* **12** 8777
- [61] Shi Z, Debenedetti P G, Stillinger F H and Ginart P 2011 *J. Chem. Phys.* **135** 084513
- [62] Sengupta S, Vasconcelos F, Affouard F and Sastry S 2011 *J. Chem. Phys.* **135** 194503
- [63] Hu Y-C, Schroers J, Shattuck M D and O'Hern C S 2019 *Phys. Rev. Mater.* **3** 85602
- [64] Pueblo C E, Sun M and Kelton K F 2017 *Nat. Mater.* **16** 792
- [65] Chatteraj J and Ciamarra M P 2020 *Phys. Rev. Lett.* **124** 028001
- [66] Landes F P, Biroli G, Dauchot O, Liu A J and Reichman D R 2020 *Phys. Rev. E* **101** 010602
- [67] Sun D Y and Gong X G 1998 *Phys. Rev. B* **57** 4730
- [68] Noya E G, Doye J P K and Calvo F 2006 *Phys. Rev. B* **73** 125407
- [69] Cao C R, Huang K Q, Shi J A, Zheng D N, Wang W H, Gu L and Bai H Y 2019 *Nat. Commun.* **10** 1966
- [70] Hoang V V and Ganguli D 2012 *Phys. Rep.* **518** 81
- [71] Li F C, Liu T, Zhang J Y, Shuang S, Wang Q, Wang A D, Wang J G and Yang Y 2019 *Mater. Today Adv.* **4** 100027

- [72] Duncan J, Wu Q, Promislow K and Henkelman G 2014 *J. Chem. Phys.* **140** 194102
- [73] Bonfanti S and Kob W 2017 *J. Chem. Phys.* **147** 204104
- [74] Miao Y 2018 *J. Chem. Phys.* **149** 072308
- [75] Ercolessi F and Adams J B 1994 *Europhys. Lett.* **26** 583
- [76] Doye J P K 2003 *J. Chem. Phys.* **119** 1136
- [77] Starace A K, Cao B, Judd O H, Bhattacharyya I and Jarrold M F 2010 *J. Chem. Phys.* **132** 034302
- [78] Dyre J C 2006 *Rev. Mod. Phys.* **78** 953
- [79] Sun D, Shang C, Liu Z and Gong X 2017 *Chin. Phys. Lett.* **34** 026402
- [80] Li X Y, Sun D Y and Gong X G 2019 *Phys. Lett. A* **383** 2604
- [81] Jellinek J, Beck T L and Berry R S 1986 *J. Chem. Phys.* **84** 2783
- [82] Mousseau N, Barkema G T and De Leeuw S W 2000 *J. Chem. Phys.* **112** 960
- [83] Giovambattista N, Buldyrev S V, Starr F W and Stanley H E 2003 *Phys. Rev. Lett.* **90** 085506
- [84] Bauer T, Lunkenheimer P and Loidl A 2013 *Phys. Rev. Lett.* **111** 225702
- [85] Karmakar S, Dasgupta C and Sastry S 2016 *Phys. Rev. Lett.* **116** 085701
- [86] Yu H-B, Richert R and Samwer K 2016 *J. Phys. Chem. Lett.* **7** 3747
- [87] Trygubenko S A and Wales D J 2004 *J. Chem. Phys.* **121** 6689
- [88] Trachenko K, Dove M T, Hammonds K D, Harris M J and Heine V 1998 *Phys. Rev. Lett.* **81** 3431
- [89] Zhang H, Kalvapalle P and Douglas J F 2010 *Soft Matter* **6** 5944
- [90] Yang Y, Zhang H and Douglas J F 2014 *ACS Nano* **8** 7465
- [91] Smith H L *et al* 2017 *Nat. Phys.* **13** 900